Competition between normal and intruder states inside the "Island of Inversion"

Vandana Tripathi[1], S.L. Tabor[1], P.F. Mantica[2,3], Y. Utsuno[4], P. Bender[1], J. Cook[2], C.R. Hoffman[1], Sangjin Lee[1], T. Otsuka[5,6], J. Pereira[2], M. Perry[1], K. Pepper[1], J. Pinter[3], J. Stoker[3], A. Volya[1], D. Weisshaar[2]
[1]*Department of Physics, Florida State University, Tallahassee, Florida 32306, USA*
[2]*National Superconducting Cyclotron Laboratory, Michigan State University, East Lansing, Michigan 48824, USA*
[3]*Department of Chemistry, Michigan State University, East Lansing, Michigan 48824, USA*
[4]*Japan Atomic Energy Agency, Tokai, Ibaraki 319-1195, Japan*
[5]*Dept. of Physics and Center for Nuclear Study, University of Tokyo, Hongo, Tokyo 113-0033, Japan*
[6]*RIKEN, Hirosawa, Wako-shi, Saitama 351-0198, Japan*
(Dated: March 9, 2007)

The β^- decay of the exotic ^{30}Ne ($N = 20$) is reported. For the first time, the low-energy level structure of the *N=19*, ^{30}Na ($T_Z = 4$), is obtained from β-delayed γ spectroscopy using *fragment*-β-γ-γ coincidences. The level structure clearly displays "inversion", *i.e*, intruder states with mainly $2p2h$ configurations displacing the normal states to higher excitation energies. The good agreement in excitation energies and the weak and electromagnetic decay patterns with Monte Carlo Shell Model calculations with the SDPF-M interaction in the *sdpf* valence space illustrates the small $d_{3/2}$ - $f_{7/2}$ shell gap. The relative position of the *normal dominant* and *intruder dominant* excited states provides valuable information to understand better the $N = 20$ shell gap.

PACS numbers: 23.20.Lv, 23.40.-s, 21.60.Cs, 27.30.+t

The anomalously large binding energies of neutron-rich ^{31,32}Na observed by Thibault *et al.*, [1] in 1975 offered a tantalizing glimpse into a new era in nuclear structure physics – one which saw the collapse of the conventional shell model. The textbook picture of fixed shell gaps and magic numbers was challenged as it was realized that the shell gaps could evolve, as a result of the shifting of single particle levels in nuclei with a large excess of neutrons, due to the spin-isospin dependence of the NN interaction. The term "Island of Inversion" was applied by Warburton [2] to a region of nuclei with $Z = 10 - 12$ and $N = 20 - 22$ due to their tendency toward prolate deformation despite the spherical driving force of the $N = 20$ magic number. Today we understand this unexpected deformation as a result of strong intruder configurations in the ground states of these nuclei, a consequence of the reduced $N = 20$ shell gap [3].

Although there is a consensus, both theoretically and experimentally, about the inclusion of fp configurations in the $N = 20$ isotones for $Z = 10 - 12$, the same cannot be said about the competition between $0p0h$ and $2p2h$ configurations for nuclei with $N < 20$ or about the degree of mixing between the various configurations. Both these depend critically on the $1d_{3/2} - f_{7/2}$ gap and to some extent on the $1f_{7/2} - p_{3/2}$ gap. Different nucleon-nucleon effective interactions used in current nuclear structure models give predictions which smear the 'island of inversion' to a larger or smaller extent. That used in the Monte Carlo Shell Model (MCSM) calculations by Utsuno *et al.*, [4, 5] creates the smallest $1d_{3/2} - fp$ gap as a function of Z (1.2 MeV for ^{28}O to 4.4 MeV for ^{34}S) and, thus, an enlarged 'island of inversion' and enhanced intruder mixing. Only experiments can select between the available models, a job rendered difficult due to the low luminosity of these exotic nuclei.

In this Letter, we report how a detailed spectroscopic study of ^{30}Na ($N = 19$) presents evidence for normal- and intruder-dominant states at low excitation energy and provides the first comprehensive look at their competition for a Na isotope inside the 'island of inversion', shown to start at $N = 18$ for Na [6]. The excited levels of ^{30}Na up to the neutron separation energy were populated following the β^- decay of ^{30}Ne ($N = 20$). The selectivity of allowed β decay from a spin 0^+ nucleus provides firm J^π assignments. The knowledge gained of the alteration in nuclear structure due to the large excess of one type of particle provides an excellent opportunity to understand the isospin-dependent part of the interaction in the nuclear medium. In particular, the structure of ^{30}Na, with an unpaired neutron close to $N = 20$, is predicted to be particularly sensitive to the $1d_{3/2} - f_{7/2}$ gap and thus provides a valuable test of the effective interaction [7].

The β^- decay of ^{30}Ne was investigated at the National Superconducting Cyclotron Laboratory (NSCL) at Michigan State University. A 140 MeV/nucleon ^{48}Ca^{20+} beam of $\sim$ 75 pnA was fragmented in a 752 mg/cm^2 Be target located at the object position of the A1900 fragment separator, used to disperse the fragments according to their A/Z. A 300 mg/cm^2 wedge-shaped Al degrader placed at the intermediate image of the A1900, allowed to separate the transmitted fragments according to Z. The magnetic rigidities of the A1900 magnets were set to 4.7856 Tm and 4.6558 Tm to select the ^{30}Ne ions. With a momentum acceptance of 2% for the A1900, the yield of ^{30}Ne was $\approx 0.09\ s^{-1}pnA^{-1}$ at the Beta Counting System (BCS) [8]. The secondary fragments were unambiguously identified by a combination of energy loss and time-of-flight information and passed through a 2.6 mg/cm^2 Al degrader before implantation in the 40 x 40 Double-sided Si micro-Strip Detector (DSSD). The DSSD, part of the

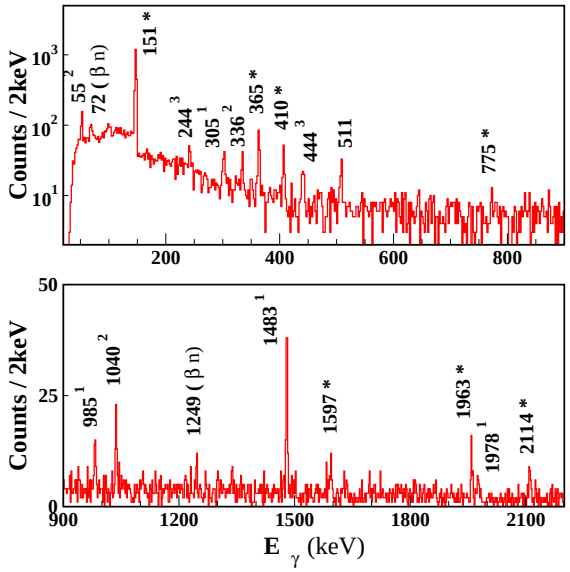

FIG. 1: (Color online) γ spectrum for events within the first 50 ms after a β^- correlated ^{30}Ne implant. The γ rays assigned to ^{30}Na (asterisk) and transitions in the β-n decay daughter, ^{29}Na, are indicated. Other transitions originate from daughter and grand daughter activity, 1: ^{30}Mg; 2: ^{29}Mg; 3: ^{30}Al.

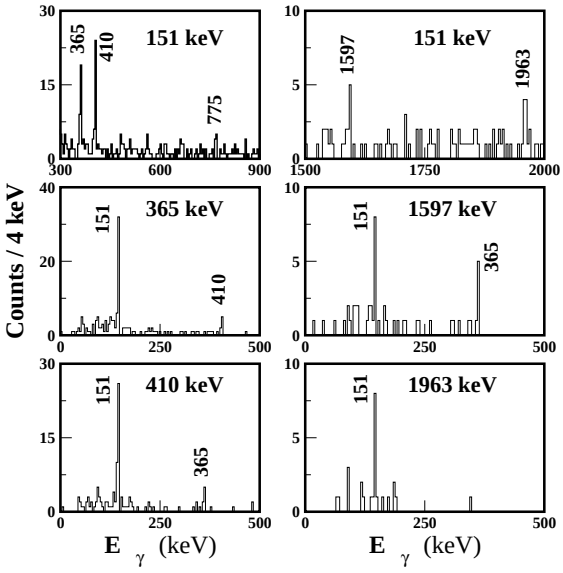

FIG. 2: $^{30}Ne - \beta - \gamma - \gamma$ coincidences, gating γ indicated.

BCS, was used to detect both the high-energy fragments and the subsequent low-energy decay products. Each recorded event had a time stamp generated by a free running clock. The details of the experimental setup were similar to those in our previous investigation of ^{28,29}Na [6, 9], except that 16 detectors of the Segmented Germanium Array (SeGA) [10] were used instead of 12, giving 25% higher γ-detection efficiency.

The γ rays observed up to 50 ms after implantation of a ^{30}Ne ion, correlated with a decay event, are shown in Fig. 1. Seven γ lines are identified to correspond to transitions in ^{30}Na, indicated in Fig. 1. Only the 151 keV had been reported before [11]. All but the 2114 keV line are in coincidence with the 151 keV (see Fig. 2), which satisfies the energy sum rule. The 365- and 410 keV transitions are seen to be in mutual coincidence and coincident with the 151 keV γ line, which along with the coincidences observed between the 365 keV and 1597 keV transitions, implies four excited states at 151-, 516-, 924- and 2114 keV. The 2114 keV level is further supported by its direct decay to the ground state as well as coincidences to show its decay to the 151 keV state. Based on the fragment-β-γ -γ coincidences and the energy and intensity sum rules, the first level scheme of ^{30}Na has been constructed following the β^- decay of ^{30}Ne (Fig. 3).

The absolute intensities of the bound levels populated in the β^- decay were calculated using the measured SeGA efficiency and the total number of ^{30}Ne decay events, 127(*14*) x 10^2, obtained from the intensities of γ transitions in ^{30}Mg, consistent with that obtained from a fit to the decay curve. The P_n and P_{2n}, expected to be significant in neutron rich nuclei, were estimated to be 12.6(*35*)% and 8.9(*23*)% respectively, from the intensities of transitions in the grand daughter nuclei, ^{30}Mg, ^{29}Mg, and ^{28}Mg, populated in $0n$, $1n$, and $2n$ emission. This is consistent with the adopted value of $< 26\%$ [12]. The decay curve in coincidence with the 151 keV transition in ^{30}Na was also used to extract the decay half life. The half life obtained is 7.3(*3*) ms (see Fig. 4), in agreement with the adopted value, 7(*2*) ms [12]. The log *ft* values for the observed states were calculated from the absolute intensities, the measured half-life and the Q_{β^-} value [13], according to Ref. [14] (ignoring the weak unobserved transitions) and are listed in Table 1.

Allowed β transitions from the 0^+ ground state of ^{30}Ne will populate only 1^+ states in the daughter ^{30}Na. The log *ft* values for the β-decay branches to the 151-, 924-, and 2114 keV states (4.03 to 4.84) imply allowed β transitions. Thus a firm assignment of $J^\pi = 1^+$ is made to these three states. The ground state of ^{30}Ne, with $N = 20$, is known to have a dominance of fp intruder configurations [15]. The most likely β^- decay scenario from such a $2p2h$ state is the conversion of one $0d_{3/2}$ neutron into a $0d_{5/2}$ proton, creating a $2p2h$ state in ^{30}Na. This would lead to stronger β branches (lower log *ft*) to the intruder-dominant 1^+ states in ^{30}Na. The observed strong branches to the 151- and 2114 keV states thus demonstrates their intruder dominance, while the relatively weaker branch to the 924 keV state suggests a purer *sd* structure of this state.

Shell model calculations carried out in the *sd* shell with the Universal (USD) interaction [16] predict only two 1^+ states below 3 MeV at 66 and 2511 keV. This along with

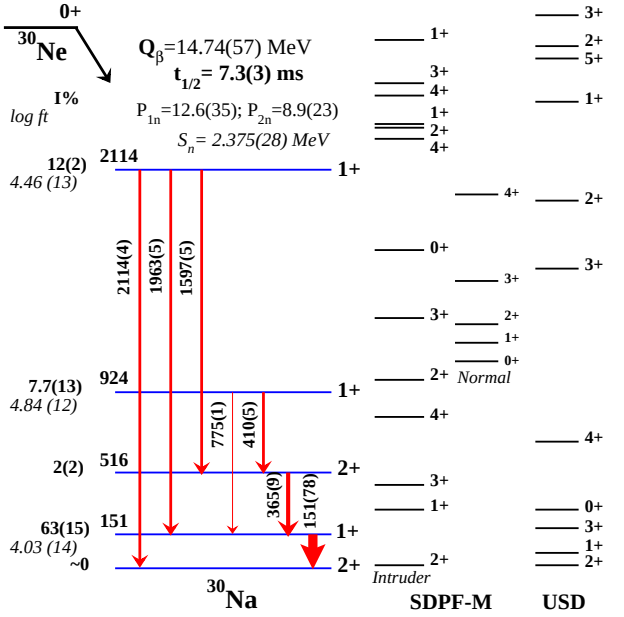

FIG. 3: (Color online) Experimental and theoretical level schemes for ^{30}Na (For MCSM, levels from 0^+ - 4^+ only are shown). Energies are in keV. Absolute intensities for the γ transitions (%) are indicated. The ground state of ^{30}Na is 2^+ [20] consistent with negligible beta branching.

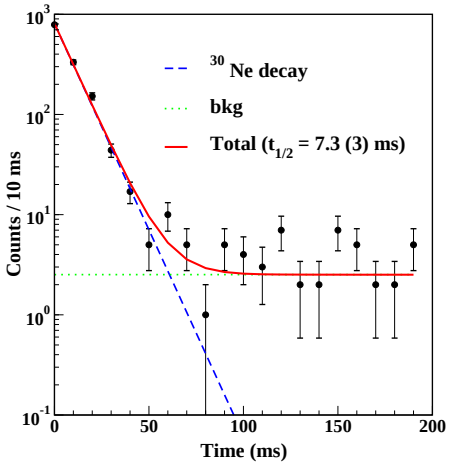

FIG. 4: (Color online) Time spectra for ^{30}Ne decay in coincidence with the 151 keV γ, fitted with a decaying exponential and a constant background to extract the half-life of ^{30}Ne.

the discrepancy in predicting the quadrupole moment of the ground state of ^{30}Na, highlights the limitation of the pure *sd* model space for this $N = 19$ nucleus. The measured quadrupole moment of ^{30}Na [17], is reproduced by the MCSM calculations [7] predicting 98% $2p2h$ configuration of the ground state. Hence states with intruder character at low excitation energies are expected in ^{30}Na.

The MCSM calculations with the SDPF-M interaction [7], which gives a narrow $N = 20$ shell gap (3.3 MeV) for Na, were performed in the $sd-p_{3/2}f_{7/2}$ space. These calculations incoporate mixing between all possible configurations. The excited states of ^{30}Na, their B(GT) values (no quenching assumed) and the electromagnetic transition strengths between the states were obtained.

The MCSM calculations predict four bound 1^+ states at 310-, 1210-, 2380-, and 2820 keV (Table 1 and Fig. 3). The lowest two calculated 1^+ states, though located higher in energy than the experimental ones at 151 keV and 924 keV, correspond well in their log ft values and γ decay. The experimental 2114 keV state agrees better in energy with the 2380 keV level, but its log ft value and γ decay branches correspond to those of the predicted 1^+ state at 2820 keV. In the latter and more likely identification, the experimental non observation of a state corresponding to 2380 keV would result from its ~5 times weaker population than the 2820 keV implied by the larger calculated log ft value. The 516 keV state is not directly populated by β decay, excluding a 1^+ assignment. The decay of the 516 keV state only to the 1^+ state, excludes $J^\pi = 3^+$, as it would favor a pure low-energy E2 over a higher energy M1 decay. Hence the possible candidate is the SDPF-M 2^+ state at 980 keV, predicted to decay almost 100% to the lowest 1^+ level, as does the 516 keV state (Table 1).

Prior studies of ^{30}Na, by intermediate-energy Coulomb excitation at the NSCL [18] and the (p,p′) reaction at RIKEN [19] measured γ rays of 433(16) and 403(18) keV respectively. Though close in energy to the 410 keV from the present work, they are unlikely to represent the same transition as it would require a multi-step decay process involving the 365 keV and 151 keV transitions, not seen in Refs. [18, 19]. The predicted 3^+ SDPF-M state at 430 keV remains the most likely identification. The 360(13) keV line observed in neutron knockout from ^{31}Na [19] could correspond to the 365 keV line reported here.

An analysis of the wave functions of the predicted levels in MCSM calculations reveals that the second 1^+ state at 1210 keV is dominated by $0p0h$ configurations, whereas the other three 1^+ states have almost pure intruder configurations, mainly $2p2h$ with ~ 1% $4p4h$ (see Table 1). This fits perfectly with the experimental picture, the 151 keV and 2114 keV states with smaller logft values as dominant $2p2h$ 1^+ states while the 924 keV state with a smaller branch as the dominant $0p0h$. The prediction of no strong connecting transitions between 2114 keV - 924 keV and 924 keV - 151 keV states, corroborated well by experimental data further projects their different character. Thus a clear 'inversion' is observed, the first excited state with dominant *sd* configuration is at 924 keV, lying above many intruder dominated states. The location of this 'normal' excited state, observed for the first time in exotic Na isotopes, is extremely important to determine exactly the $sd - fp$ shell gap. The ground state properties, on the other hand, can provide

TABLE I: Excitation energies, logft values and γ-branching ratios for the observed levels in ^{30}Na, and the predictions of the MCSM calculation with the SDPF-M interaction [7]. For MCSM, the probability of 2p2h contribution is also indicated.

Exp.				SDPF-M				
E_x (keV)	J^π	log ft	γ-branching(%)	E_x (keV)	J^π	log ft[a]	γ-branching(%)[b]	2p2h(%)
151(*1*)	1^+	4.03(*14*)	0(100)	310	1^+	3.9	0(100)	98
516(*1*)	2^+	-	151(100)	980	2^+	-	310(99.8)	87
924(*1*)	1^+	4.84(*12*)	516(83); 151(17)	1210	1^+	4.9	980(64); 310(32); 0(4)	23
2114(*2*)	1^+	4.46(*13*)	516(36); 151(36); 0(28)	2380	1^+	4.9	1210(1); 980(7); 310(88); 0(4.5)	98
-	-	-	-	2820	1^+	4.2	1210(0.1); 980(36); 310(40); 0(24)	96

[b]ground state of ^{30}Ne had 4% of $0p0h$, 74% of $2p2h$ and 22% of $4p4h$ configuration
[b]γ-ray energies taken from experimental data

only the upper limit.

The situation is different for the less exotic ^{29}Na [6], where the intruder dominated states occur at higher excitation energy, as seen from Fig. 5. The 1249 keV level is assigned a $J^\pi = 3/2^+$ from the present work, assuming its population in β-n emission (Fig. 1) from an unbound 1^+ in ^{30}Na by a $l = 0$ neutron (most probable due to the low energy). This corresponds to the SDPF-M state at 1760 keV and is the first excited state with dominant intruder configuration in ^{29}Na. The comparison of the lowest excitations in ^{29,30}Na thus illustrates the mechanism of intrusion, *i.e*, states with dominant intruder configuration moving to lower excitation energies by gaining correlation energy, as the neutron number increases [7].

To recapitulate, a comparison of the excited states, weak and electromagnetic branching ratios in the β^- decay of ^{30}Ne to ^{30}Na with shell model predictions in the $sd - f_{7/2}p_{3/2}$ space, clearly demonstrates the 'inversion', *i.e.* a number of *intruder dominated* states lie below the lowest *normal dominant* state. The decay branches agree surprisingly well, though the calculations tend to overpredict the excitation energies, a trend also seen in ^{29}Na. For the first time, excited 'normal' and 'intruder' states have been unambiguously identified inside the 'island of inversion'. Their relative position provides valuable information for better determining the $d_{3/2}$ - $f_{7/2}$ gap and thus the evolution of shell structure with isospin.

The authors appreciate the NSCL operations staff for their help. This work was supported by the NSF grants PHY-01-39950 and PHY-06-06007 and in part by a Grant-in-Aid for Specially Promoted Research (13002001) from the MEXT of Japan.

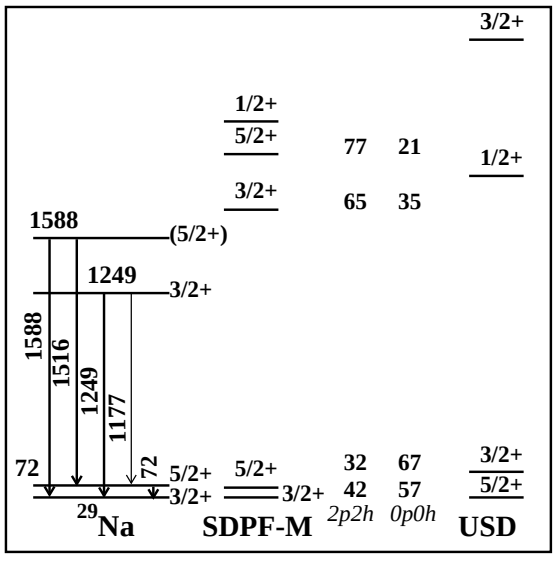

FIG. 5: Partial level scheme of ^{29}Na from Ref. [6]. The J^π assignments to the states at ∼1.5 MeV are from the present work. Configuration of the levels ($2p2h$ and $0p0h$) obtained with the SDPF-M interaction are listed (in %).

[1] C. Thibault *et al.*, Phys. Rev. C **12**, 644 (1975).
[2] E. K. Warburton, J. A. Peeker, and B. A. Brown, Phys. Rev. C **41**, 1147 (1990).
[3] T. Otsuka *et al.*, Phys. Rev. Lett. **87**, 082502 (2001).
[4] Y. Utsuno *et al.*, Phys. Rev. C **60**, 054315 (1999).
[5] Y. Utsuno *et al.*, Phys. Rev. C **64**, 011301(R) (2001).
[6] V. Tripathi *et al.*, Phys. Rev. Lett. **94**, 162501 (2005).
[7] Y. Utsuno *et al.*, Phys. Rev. C **70**, 044307 (2004).
[8] J. I. Prisciandaro *et al.*, Nucl. Instrum. Methods Phys. Res., Sect.A **505**, 140 (2003).
[9] V. Tripathi *et al.*, Phys. Rev. C **73**, 054303 (2006).
[10] W. F. Mueller *et al.*, Nucl. Instrum. Methods Phys. Res., Sect. A **466**, 492 (2003).
[11] A. T. Reed *et al.*, Phys. Rev. C **60**, 024311 (1999).
[12] ENSDF datebase: http://www.nndc.bnl.gov/ensdf/
[13] G. Audi *et al.*, Nucl. Phys. A**729** (2003).
[14] N. B. Gove and M. J. Martin, Nucl. Data Tables A **10**, 205 (1971).
[15] Y. Yanagisawa *et al.*, Phys. Lett. B **566**, 84 (2003).
[16] B. A. Brown and B. H. Wildenthal, Annu. Rev. Nucl. Part. Sci. **38**, 29 (1998).
[17] M. Keim, Proc. Conf. on Exotic Nuclei and Atomic masses, Bellaire, Michigan, June 23-27, 1998, p50.
[18] B. V. Pritychenko *et al.*, Phys. Rev. C **66**, 024325 (2002).
[19] Z. Elekes *et al.*, Phys. Rev. C **73**, 044314 (2006).
[20] G. Huber *et al.*, Phys. Rev. C **18**, 2342 (1978).